atmosphere

MDPI

Article

Coupling MATSim and the PALM Model System—Large Scale Traffic and Emission Modeling with High-Resolution Computational Fluid Dynamics Dispersion Modeling

Janek Laudan [1,*], Sabine Banzhaf [2], Basit Khan [3] and Kai Nagel [1]

[1] Institute of Land and Sea Transport Systems, Transport Systems Planning and Transport Telematics, Technische Universität Berlin, Kaiserin-Augusta-Allee 104-106, 10365 Berlin, Germany; nagel@vsp.tu-berlin.de
[2] Institute of Meteorology, Tropospheric Environmental Research, Freie Universität Berlin, Carl-Heinrich Becker-Weg 6-10, 12165 Berlin, Germany; sabine.banzhaf@met.fu-berlin.de
[3] Mubadala Arabian Center for Climate and Environmental Sciences (ACCESS), New York University Abu Dhabi, Abu Dhabi P.O. Box 129188, United Arab Emirates; basit.khan@nyu.edu
* Correspondence: laudan@tu-berlin.de; Tel.: +49-30-23308

Abstract: To effectively mitigate anthropogenic air pollution, it is imperative to implement strategies aimed at reducing emissions from traffic-related sources. Achieving this objective can be facilitated by employing modeling techniques to elucidate the interplay between environmental impacts and traffic activities. This paper highlights the importance of combining traffic emission models with high-resolution turbulence and dispersion models in urban areas at street canyon level and presents the development and implementation of an interface between the mesoscopic traffic and emission model MATSim and PALM-4U, which is a set of urban climate application modules within the PALM model system. The proposed coupling mechanism converts MATSim output emissions into input emission flows for the PALM-4U chemistry module, which requires translating between the differing data models of both modeling systems. In an idealized case study, focusing on Berlin, the model successfully identified "hot spots" of pollutant concentrations near high-traffic roads and during rush hours. Results show good agreement between modeled and measured NO_x concentrations, demonstrating the model's capacity to accurately capture urban pollutant dispersion. Additionally, the presented coupling enables detailed assessments of traffic emissions but also offers potential for evaluating the effectiveness of traffic management policies and their impact on air quality in urban areas.

Keywords: traffic simulation; emission modeling; air pollution; pollution hot spot; CFD

Citation: Laudan, J.; Banzhaf, S.; Khan, B.; Nagel, K. Coupling MATSim and the PALM Model System—Large Scale Traffic and Emission Modeling with High-Resolution Computational Fluid Dynamics Dispersion Modeling. *Atmosphere* **2024**, *15*, 1183. https://doi.org/10.3390/atmos15101183

Academic Editor: Mingliang Fu

Received: 29 August 2024
Revised: 23 September 2024
Accepted: 26 September 2024
Published: 30 September 2024

1. Introduction

In light of the burgeoning urbanization trend, with over half of the global population presently dwelling in urban areas [1], the concern regarding air pollution has intensified significantly. Prolonged exposure to air pollution can lead to adverse effects on diverse physiological systems, encompassing the respiratory, cardiovascular, metabolic, and neurological functions [2]. Despite a decline in premature deaths in Europe, air pollution remains a significant health concern [3,4].

One of the main sources of urban air pollution in cities is car traffic, as shown by studies measuring individual exposure [5,6] or by applying statistical methods [7]. In addition, Ehrnsperger and Klemm [8] and von Schneidemesser et al. [9] find that pollutant concentrations correspond to observed traffic patterns in urban environments, making reduction in traffic-induced emissions a priority to mitigate pollutant concentrations and improve the health situation of the urban population.

Developing mitigation strategies for the impact of traffic emissions requires understanding the relation between traffic and its environmental impact. Gürbüz et al. [10]

investigate the interplay between fuel consumption and the environmental impact during the COVID-19 lockdown in Turkey. However, predicting the efficiency of future policies requires the application of traffic, emission, and dispersion models to simulate various traffic scenarios and their environmental impacts. The first step in modeling this relation is to compute emissions from traffic using an emission model. Forehead and Huynh [11], Mądziel [12] and Ma et al. [13] provide a comprehensive overview of available traffic emission models, which can be divided into two categories:

1. **Aggregate**—traffic emissions are based on aggregated parameters such as average vehicle speed on links or overall vehicle distance traveled. Important models are, for example, MOBILE6 (an emissions model for mobile sources) [14], MOVES (Motor Vehicle Emission Simulator) [15], COPERT (Computer Program to Calculate Emissions from Road Transport) [16] or ARTEMIS (Assessment and Reliability of Transport Emission Models and Inventory Systems) [17];
2. **Microscopic**—emitted pollution is calculated at the vehicle level, considering attributes such as vehicle speed, acceleration, engine type and others. Prominent models are CMEM (Comprehensive Modal Emission Model) [18], VT-MICRO (Vehicle Trajectory-based Microscopic Model) [19], EMIT (Environmental Model of Individual Traffic) [20] and POLY (Microscale Emission Model Incorporating Acceleration and Deceleration) [21].

Aggregate and microscopic emission models are best combined with corresponding categories of traffic models as input for emission calculations. Aggregate models work well with aggregate traffic models while microscopic emission models require input on the vehicle level which requires the use of micro- or mesoscopic traffic models [11,13].

Once traffic emissions are properly modeled, a dispersion model can be used to investigate the dispersion of pollution in the urban environment. Johnson [22] provides an introduction into dispersion models in general, while Vardoulakis et al. [23] and Forehead and Huynh [11] list traffic-related dispersion models. These include Line-Source Models such as CALINE [24], RLINE (a dispersion model for near-road applications) [25] and operational models such as OSPM (Operational Street Pollution Model) [26], ADMS (Atmospheric Dispersion Modeling System) [27], or IMMIS (Integrated Model for the Management of Traffic-related Emissions) [28] which parameterize turbulence in street canyons and even include atmospheric chemistry reactions.

More accurate results are to be expected from CFD (Computational Fluid Dynamics) models of which, in addition to the reviews above, Tominaga and Stathopoulos [29] and Khan et al. [30] provide an overview of models capable of simulating emission dispersion. In contrast to parameterized models, CFD models are based on atmospheric turbulent fluid dynamics, solving differential equations to determine atmospheric pressure and flow within discrete raster cells of the simulated domain [31]. By simulating atmospheric turbulence and solving a transport equation together with a model driven, chemical mechanism, the pollutant concentrations and dispersion can be calculated [32]. For emission calculations, either RANS (Reynolds-Averaged Navier–Stokes) or LES (Large Eddy Simulation) models are used, of which LES requires more computational resources but can provide more accurate results regarding wind flow around obstacles like buildings [33].

Several studies have applied traffic induced emissions with dispersion models. Forehead and Huynh [11] include a list of applications where most of the studies use aggregate emission and parameterized dispersion models (e.g., Batterman et al. [34]) or simulate small domains using microscopic emission and dispersion models (e.g., Ioannidis et al. [35], Grumert et al. [36]). Liang et al. [32] provide a more recent overview of coupling CFD dispersion and traffic emission models. They find that "*CFD models are generally used for pollutant dispersion studies at the street or micro-district level*" [32] due to the requirements on computational resources. In contrast to the majority of studies, Sanchez et al. [37] and San José et al. [38] present high-resolution emission dispersion calculation in real urban environments. Both studies use high-resolution traffic models to calculate traffic emissions and CFD-RANS models for dispersion simulation.

Adding to the cited work, this paper describes the development of an interface between the mesoscopic traffic and emission model MATSim (Multi-Agent Transport Simulation) [39] and the urban climate simulation model PALM-4U [40], which was developed as part of the UC_2 (Urban Climate Under Change) [41] project. MATSim simulates traffic dynamics across large regions, accommodating millions of simulated people. Employing a mesoscopic approach, MATSim captures individual vehicles without explicitly modeling vehicle dynamics such as acceleration or following behavior, which enables the calculation of traffic induced emissions for large urban areas. PALM-4U, a CFD model which is designed to be scaled onto HPC (High-Performance Computing) infrastructure, is able to simulate chemical transformation, advection, and deposition of air pollutants for large realistically shaped urban areas [40]. By operating in LES mode, it provides an accurate representation of atmospheric turbulence, especially in urban canopies with complex building geometries.

While many studies rely on either aggregate emission models with parameterized dispersion or high-resolution simulations limited to smaller domains [32], our approach integrates a large-scale, behavior-based traffic model with a high-resolution CFD model. This coupling enables the simulation of traffic emissions on the scale of large urban districts while maintaining the accuracy required to model turbulence and chemical processes in street canyons. We demonstrate the value of this approach in an idealized case study located in Berlin, focusing on the identification of pollution "hot spots"—areas where pollutant concentrations are particularly high. Coupling both models provides a powerful tool for improving urban air quality management and testing the effectiveness of traffic policies.

2. Materials and Methods

The coupling of the traffic simulation MATSim and the CFD model PALM-4U follows the data flow presented in Figure 1. Starting with the standard output of a MATSim simulation run, the corresponding traffic emissions are calculated using the methodology described in Section 2.2. Based on the calculated traffic emissions, a chemistry driver file is generated using the coupling methodology presented in this paper. The generated chemistry driver along with other input files is used as input for a PALM-4U simulation run.

The proposed coupling mechanism is built on top of existing technology, which is described in the following section.

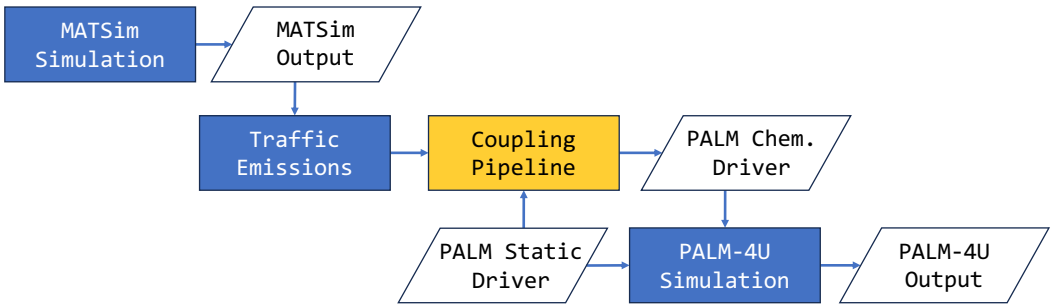

Figure 1. Data flow of the model integration: Traffic emissions calculated based on output of a MATSim simulation are converted into a PALM chemistry driver. The resulting driver is part of the input for a subsequent PALM-4U simulation.

2.1. Traffic Simulation

MATSim is an open-source traffic simulation which models travelers as individual simulated people [39]. Each simulated person maintains a daily plan of activities which it tries to accomplish throughout the day. To reach activities of their plan, simulated people travel along a simulated road network, competing for limited resources with other simulated people. Each simulated person tries to maximize its utility by adapting to the limited traffic supply. The optimization of utility is done in the form of a co-evolutionary algorithm where the same day is iterated multiple times. One iteration includes three steps:

1. During the mobility simulation, simulated people execute their individual plans while interacting with other simulated people. To support large-scale scenarios, vehicles are simulated using a queue model, omitting calculation of computationally complex vehicle dynamics or car following behavior. However, the queue model accounts for congestion and spill back effects important for mesoscopic traffic patterns.
2. The executed plan of each simulated person is evaluated through a utility score. In general, performing activities increases the score, spending time in traffic or monetary costs, e.g., public transit fares or cost of car ownership decrease the score.
3. A fraction of all simulated people adapts their behavior by inventing new plans. This includes choosing alternative routes, switching between modes or adapting departure times. The remaining share of simulated people picks a plan from the set of plans that it has already memorized.

After a certain number of iterations, the simulation reaches an equilibrium where individual simulated people cannot improve their situation any further.

2.2. Emission Model

The MATSim framework provides an extension for emission modeling, initially developed by Hülsmann et al. [42] and later improved by Kickhöfer et al. [43]. Based on the simulated traffic dynamics, emissions are calculated using emission factors from the HBEFA (Handbook Emission Factors for Road Transport) version 4.1 database [44], which accounts for traffic situations such as road type, current traffic flow and vehicle speed, as well as vehicle properties such as vehicle type and engine type being the most important. Emissions in MATSim are calculated on a per-link and per-vehicle basis. This corresponds to the level of detail at which traffic is simulated. Once a vehicle has traversed a link in the network, corresponding emission factors are selected from the HBEFA database. The emission factors for different pollutants are multiplied with the traveled distance of the vehicle on the link and stored in the form of an emission event. As shown in Figure 2, emission events are stored in the general event log of a MATSim run, from which the simulated reality can be re-created after a simulation run has finished.

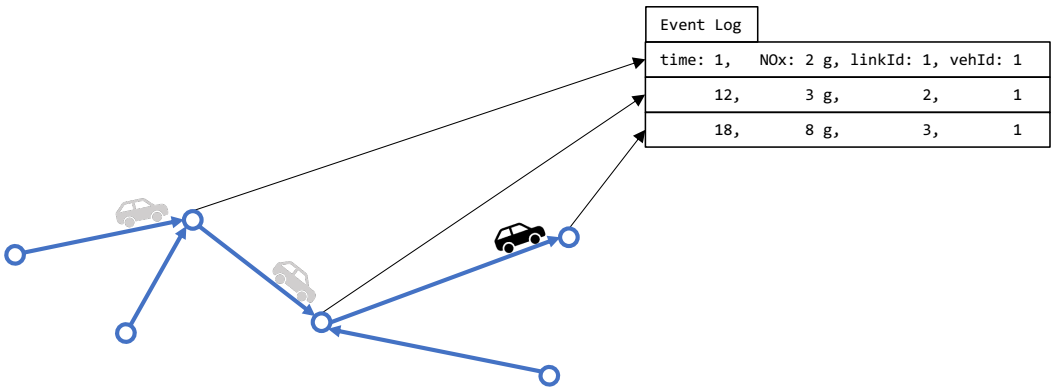

Figure 2. Example of emission calculation in the MATSim emission extension. A vehicle traverses three links on the simulation's street network, resulting in three emission events in the general event log. For simplicity, only NO_x (Nitrogen Oxides) emissions are depicted. The emission extension is capable of calculating all the pollutants HBEFA provides emission factors for.

To validate their methodology, Hülsmann et al. [42] conducted an experiment involving recorded vehicle trajectories, from which emissions were calculated using the detailed PHEM (Passenger car and Heavy-duty Emission Model) emission model with a temporal resolution of one second. The study finds significant variations in individual vehicular emissions calculated with PHEM on the same link, even under similar traffic conditions. The averaged emissions calculated from the real-world vehicle trajectories were then compared to emissions calculated, using simulated traffic in MATSim and HBEFA emission

factors, with the result that the presented emission tool is able to "*approximate emission levels that look similar to PHEM data and show similar tendencies over time of day*" [42].

Conceptually, vehicular emissions based on HBEFA emission factors reflect the average emission that a typical vehicle with the same properties in the same traffic situation on the same type of link would have produced. This is comparable to using detailed vehicle trajectories with a high-resolution, high-fidelity model such as PHEM and averaging the emissions afterward. The presented approach for calculating traffic emissions, retains the microscopic resolution of both the individual vehicles and the vehicle properties relevant for emission calculations while employing an average value for the emission outputs. In consequence, when combined with a microscopic dispersion model, hot spots with exceeding levels of pollutant concentrations are the result of structurally unfavorable traffic conditions in combination with unfavorable meteorological conditions. An investigation of vehicular emissions with a temporal and spatial resolution finer than the size of a link is not feasible with the presented coupling approach. However, a spatial resolution on the link level is sufficient for investigating traffic emissions and their effects on a regional scale.

MATSim's emission module is currently also capable of estimating pollutant concentrations on a grid of receiver points [45] using a Gaussian Blur. However, the current method ignores important aspects of dispersion modeling such as wind, obstacles, chemical reactions or the height of the boundary layer.

2.3. Dispersion and Air Chemistry Model

The urban climate simulation tool PALM-4U is a CFD model that incorporates a LES turbulence model. It allows for the simulation of atmospheric boundary layer flows, with a particular focus on urban environments [40]. Designed to scale on massively parallel computing hardware, this model is capable of simulating large domains with fine grid resolutions [46]. In PALM-4U, the urban canopy is modeled using a static driver file [40], which contains information such as topography, surface and street types, and building heights. In addition to resolving atmospheric turbulence, the PALM model system includes an atmospheric chemistry module [30] that simulates the transport, chemical reactions, and deposition of pollutants. The combination of the turbulence model with the simulation of photochemical reactions allows for detailed predictions of pollutant concentrations in urban environments, as demonstrated by Khan et al. [30], making it possible to investigate pollution hot spots with high precision.

Traffic emissions can be input into the chemistry module with varying LOD (Level of Detail). In the fully parameterized LOD 0 mode, emissions are estimated based on street types defined in the static driver file. The default LOD 1 mode provides parameterized emissions derived from annually averaged traffic volumes, with the option to incorporate temporal and spatial variations through the chemistry driver file. Finally, in LOD 2 mode, the chemistry module requires fully pre-processed emissions supplied by the chemistry driver file. The coupling method presented here utilizes LOD 2 mode to integrate traffic emissions generated by MATSim into a given PALM-4U simulation setup.

3. Implementation of Coupling Method

The coupling of traffic emissions generated using MATSim, to the urban climate model PALM-4U is achieved seamlessly through the utilization of PALM-4U's chemistry module. As presented in Figure 3, the coupling of both models is carried out by converting MATSim output data into the PALM-4U chemistry driver file format [40]. The chemistry driver file format is part of the PIDS (PALM Input Data Standard) and is the preferred way of supplying emission information needed for the PALM-4U climate simulation. As MATSim and PALM-4U are programmed in different programming languages, implementing the coupling mechanism by exchanging data via input files allows running both models independently in different computing environments.

When converting MATSim output data into the chemistry driver file format, the problem of different spatial representations and differing temporal resolutions must be resolved.

Spatial information in MATSim is modeled as vector data in Euclidean space, while the PALM model system divides the simulation domain into a regular raster where each grid cell covers a discrete volume. Results of a MATSim simulation are stored using a time step size of one second, while the PALM-4U chemistry module expects accumulated emission flows over uniform time periods. Additionally, traffic in MATSim is simulated on a network with simplified link geometries, to save computational resources, which interferes with high-resolution emission modeling. Hence, converting traffic emissions into chemistry driver input is conducted in four steps, which are also highlighted in Figure 3:

1. Mapping of detailed and simplified link geometries;
2. Temporal aggregation of traffic emissions;
3. Rasterizing of vector-based traffic emissions;
4. Writing of the driver file.

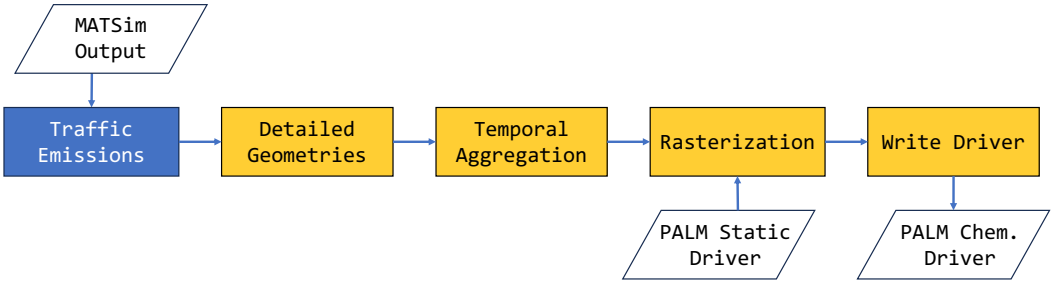

Figure 3. Data flow of the coupling pipeline. With traffic emissions generated from MATSim output data, a chemistry driver for a PALM-4U simulation is generated. The four main stages of the pipeline are executed in consecutive order: (1) mapping of detailed link geometries, (2) temporal aggregation of traffic emissions, (3) rasterization of traffic emissions, and (4) writing of the driver file.

3.1. Mapping of Detailed and Simplified Link Geometries

Traffic in MATSim is modeled on a directed graph that consists of nodes (vertices) and links (edges). The links in the network represent streets and carry essential information for the mobility simulation, such as capacity, freespeed, and the number of lanes. Nodes, on the other hand, represent intersections where vehicles can switch from one link to another. Additionally, nodes contain geographical information about the network. MATSim networks are typically generated using OSM (OpenStreetMap) data, which are filtered for street-related information and then converted into the MATSim network format. During the conversion process, the original street network geometries are simplified, keeping only nodes with intersections in the MATSim network (see Figure 4), thus reducing computational load and memory footprint during a MATSim run. To ensure correct travel times, the original length of the simplified street segment is stored as a separate length parameter on the link.

However, this abstraction is not suitable when it comes to modeling detailed traffic emissions. Simplified links might cut through occupied areas, as can be seen in Figure 4, leading to traffic emissions being emitted from within buildings. To provide accurate emission flows to the chemistry model, the emissions calculated based on simplified link geometries must be mapped onto more detailed street geometries. Since the OSM data set originally used to generate the traffic network contains the required information, a mapping between the traffic network and the original geometries is established. During network generation from OSM data, the original street geometry is stored in the form of a link attribute containing a list of (ID, x, y)-triplets, which corresponds to the data model of a MATSim network node. With this information, a MATSim network with detailed link geometries can be re-created to calculate traffic emissions while maintaining the advantages of simplified link geometries during the traffic simulation.

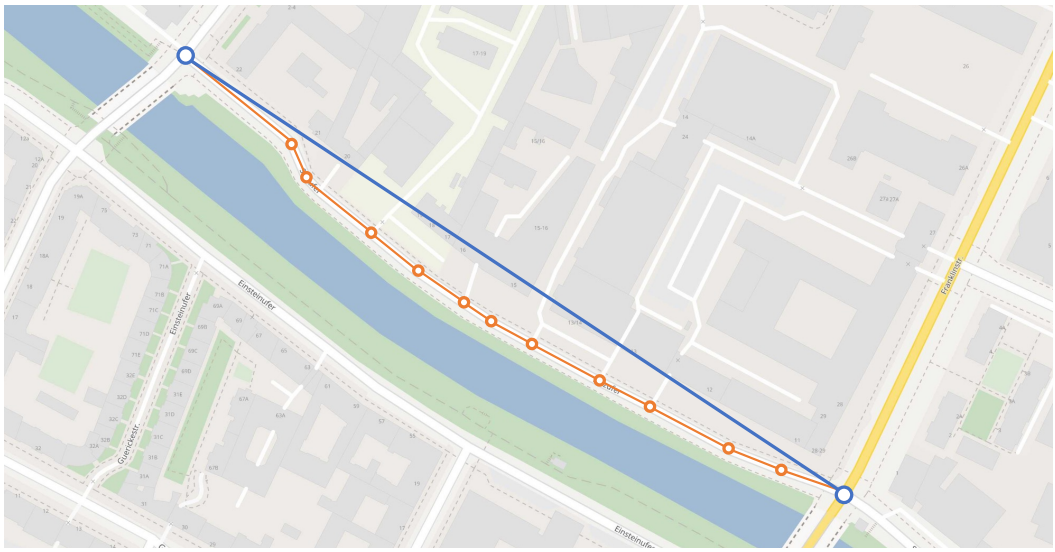

Figure 4. Example of a simplified street geometry in a MATSim network (blue) and its corresponding original geometry from OSM (orange).

3.2. Temporal Aggregation of Traffic Emissions

In the context of coupling MATSim and PALM-4U, it is important to be aware of differing time resolutions in the various steps of the modeling pipeline:

- MATSim functions at a high temporal resolution, processing data every second. This is evident as emissions in the MATSim event file are recorded with precise timestamps indicating the moment a vehicle exits a link.
- The time periods in the chemistry driver used in the idealized case study (see Section 4) are set to one hour intervals. Though, due to recent advancements, the driver format now supports arbitrary time periods, at the time the idealized case study was conducted, only one hour periods were available. During each one-hour period, emission input into the PALM-4U simulation is constant.
- The internal transport equations in PALM-4U, as well as the calculations for pollutant concentrations and dispersion, are executed on the scale of seconds.
- The temporal frequency of the model's output was set to hourly intervals for the purpose of our idealized case study.

As the temporal resolution of MATSim is one second, the produced traffic emissions must be aggregated into the time periods of the chemistry driver. Figure 5 illustrates this process with two time periods, each having a duration of one hour. All emission events with time stamps between 0 and 3600 are sorted into the time period between midnight and 1am. All other events with time stamps between 3601 and 7200 are sorted into the time period between 1 am and 2 am. Within each time period, emission events are accumulated by link. For example, in the time period between midnight and 1 am, link 2 is traversed by two vehicles each issuing 3 g of NO_x accumulating to 6 g of NO_x for link 2 during that time period. As the PALM model system uses a variable time step size in the magnitude of seconds, which is determined at runtime, the aggregated emissions from the chemistry driver are disaggregated during a PALM-4U simulation run. For each simulated time step within the same time period, the chemistry module releases a constant amount of emissions into the PALM-4U simulation domain. In the example of one hour periods, the flow of emissions released into the simulation domain changes once every hour.

As described in Section 3.1, traffic emissions must be mapped onto detailed street geometries to achieve an accurate dispersion simulation, which is also performed during the aggregation step of the conversion. According to Section 3.1, a network with detailed street geometries is generated from the additional OSM nodes stored as link attributes. During the creation of the detailed network, a mapping is introduced which associates a

simplified link with all the shorter links which were re-created from the detailed geometry information of that link. With the mapping between simplified and detailed links in place, aggregated traffic emissions for a simplified link can be distributed onto the detailed link geometries. The distribution of traffic emissions onto mapped links considers the length of each short link compared to the length of the simplified link. Although the detailed link geometries shown in Figure 4 appear longer than the simplified links used in the traffic simulation, the traveled distance used for the emission calculations is identical to the accumulated Euclidean distance of the detailed link geometries. This is because the original length of the simplified link is preserved as a separate property, and is used for the traffic model. Distributing the emissions evenly over the entire length of a link, overlooks potential variations in emissions at different points along the link. For instance, it is expected that vehicles emit more emissions toward the start and end of a link, where acceleration typically occurs. Nevertheless, this level of granularity matches the resolution at which traffic is simulated in MATSim, as discussed in Section 2.2.

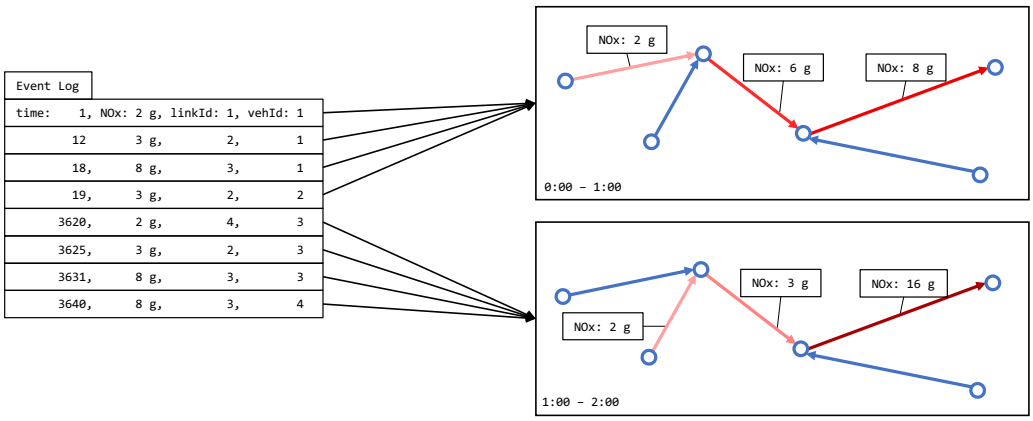

Figure 5. Aggregation step of emission events. Emission events from the event log are aggregated by time period. Within each time period, emissions of the same pollutant are aggregated by link. Links in red shades indicate that emissions were produced on those links during the respective time period. Darker shades indicate a higher amount of emissions. Blue links indicate that no emissions were produced on that link during the respective time period.

Although the detailed link geometries in Figure 4 appear to be longer than the simplified link used in the traffic simulation, the traveled distance used in the emission calculation is the same as the accumulated Euclidean distance of the detailed link geometries, as the original length of the link is preserved as separate property on the simplified link. Distributing the emissions over the entire length of a link evenly, misses potential differences in the amount of emissions emitted at different locations of a link. For example, it is to be expected that vehicles emit more emissions towards the start and the end of a link, where acceleration usually takes place. However, this corresponds to the level of detail at which traffic is simulated in MATSim and is discussed in Section 2.2.

Based on the HBEFA emission factors, MATSim generates separate values for particulate matter caused by the combustion process and particulate matter caused by other factors like breaks and tire abrasion. This is useful for studying certain policy cases, for example, the electrification of the car fleet, where particulate matter caused by the combustion process would be eliminated, but the remaining particulate matter would still be present. The PALM-4U chemistry driver file is expected to contain the sum of emissions regardless of their source, separated by species. This requirement makes the aggregation of particulate matter stemming from the combustion process and other sources necessary and is performed during the aggregation phase of the pipeline.

3.3. Rasterizing of Vector-Based Traffic Emissions

The PALM model system is a grid-based model. Therefore, the link-based emissions from MATSim have to be converted into gridded emission data for the PALM-4U simulation. The traffic emissions, which were temporally aggregated in the previous step, must be distributed onto the raster chosen for the PALM-4U simulation. One raster with emission flows is required for each time period of the chemistry driver file. The process of distributing link-based emissions onto a raster is comparable to drawing lines on a screen, where vectors are translated onto a pixel grid. As it is fast and easy to implement, Bresenham's line-drawing algorithm [47] is used as a basis to convert link based into raster-based emissions.

The implemented algorithm assumes that emissions for a certain link were emitted evenly across all cells covering that link. To determine the amount of emission per cell, the number of cells covering a link are counted in a first pass of the raster algorithm. In the second pass, the accumulated emissions for the current link are distributed evenly across all covering cells. This process is performed based on the detailed link geometries described in Section 3.1. Individual links vary in length from a few meters up to more than a hundred meters, depending on the geometry of the street they represent, as well as the distance between intersections. In comparison, a resolution between one and ten meters is typically used to conduct PALM-4U LES mode simulations in urban setups. In the case of a raster cell covering more than one link, the emissions from all links are accumulated. Figure 6 shows how the emissions from the previous example are distributed onto the raster. For the links in red, emissions were calculated for the corresponding time period. The resulting emissions are distributed onto the raster, where darker shades represent higher emission flows. Furthermore, it is visible that the raster cell with the highest emission flow covers multiple links. The described step is repeated for each time period and for each pollutant.

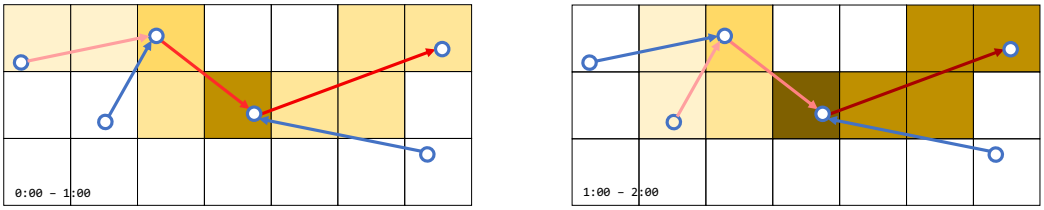

Figure 6. Rasterization step of aggregated emissions: A separate raster is produced for each time period of the simulation. Within each time period, the accumulated emissions of each link are distributed onto raster cells by the means of Bresenahm's line drawing algorithm. Red shades indicate the amount of emissions produced on a link within the respective time period, with darker colors indicating higher values. Yellow shades indicate the amount of emissions distributed on each raster cell. Darker shades indicate higher values.

The MATSim emission model calculates values for NO_x and NO_2 (Nitrogen Dioxide) based on the corresponding emission factors in the HBEFA database. An accurate chemistry simulation, however, requires distinct values for NO_2 and NO (Nitrogen Monoxide). The missing NO values are calculated by subtracting NO_2 from NO_x after the raster step of the conversion. For each time period, the raster values of NO_2 are subtracted from the NO_x raster values.

3.4. Chemistry Driver File

The transformed emission data are written into a chemistry driver file, which contains the emission information necessary to run a PALM-4U simulation. The driver file format [40] is part of the PIDS (PIDS_Chem) and contains rasterized emission information divided into uniform time periods. The file structure is based on the NetCDF standard, which was designed to accommodate multidimensional raster data. The information about time periods, species and the x, y coordinates are stored in separate indices in the file, which allows for random access by those dimensions. Based on the transformations described in

the previous sections, the chemistry driver file is populated with traffic emissions for each raster cell and each time period separated by species.

Figure 7a shows the content of a chemistry driver file for the PALM-4U model setup used in Section 4. The image shows NO_2 emission flows into the PALM-4U model setup for the time period between 8 am and 9 am for a 6.7 km times 6.7 km model domain with a 10 m grid resolution. NO_x has already been split up into NO and NO_2 by subtracting NO_2 from NO_x as described in Section 3.3. The overall pattern of emission flows corresponds to the hierarchy of the street network. Major roads, as well as the inner-city freeway, produce high traffic emission flows, while minor streets appear less pronounced. The driver file in Figure 7a additionally contains emission values for particulate matter, NO, and CO (Carbon Monoxide).

The PALM model system requires simulations to run in UTC time format. Since attributes such as sun radiation play an important role, it is crucial to know what time and date it is. MATSim, on the other hand, is date-agnostic and only counts seconds from the beginning of the simulation. Usually, a MATSim simulation begins at midnight local time, so that a conversion of MATSim time stamps into UTC time is necessary. This step is performed during the writing phase of the processing pipeline.

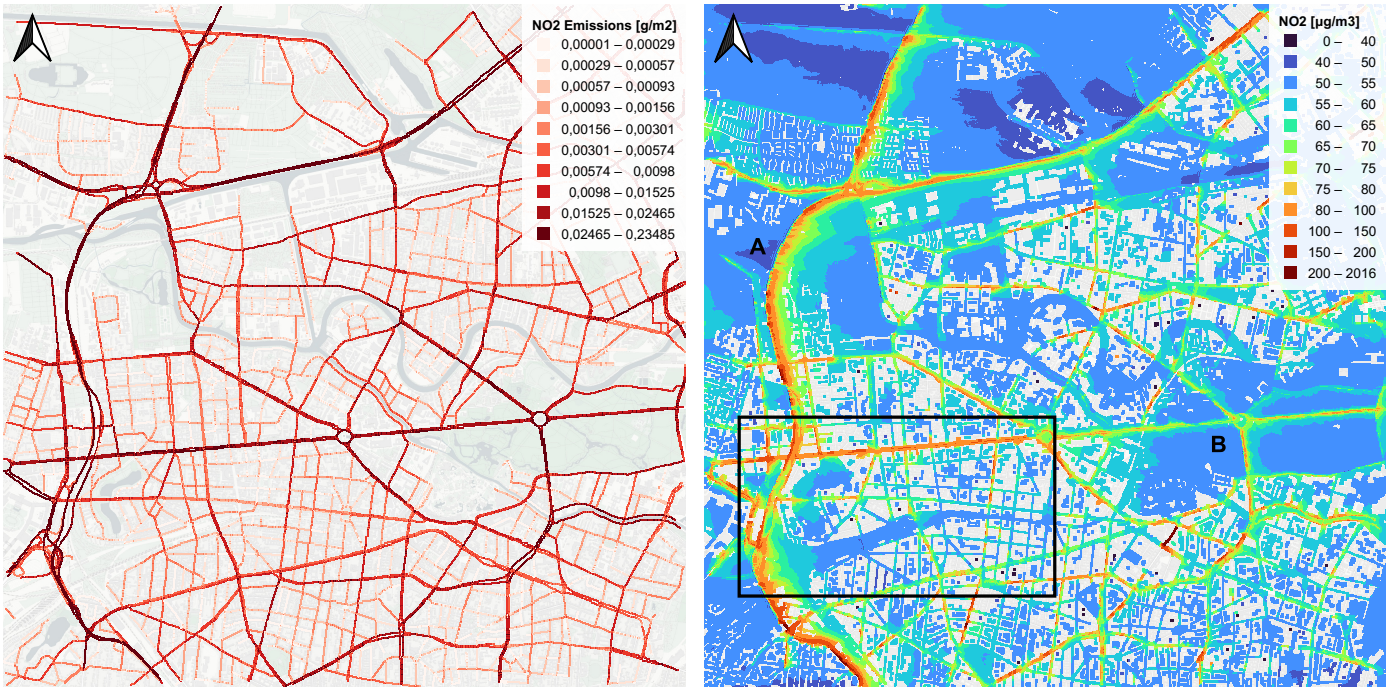

(**a**) (**b**)

Figure 7. (**a**) Rastered emission flows in g/m^2 for the period between 8 am and 9 am. Emission flows in (**a**) are the output of the MATSim emission model and the raster pipeline; NO_x has already been split into NO and NO_2. (**b**) shows the corresponding NO_2 concentrations simulated with PALM-4U for the same time period. The area of the rectangle in (**b**) corresponds to Figure 8; letters A and B highlight the effects of the wind direction explained in Section 4.3.3.

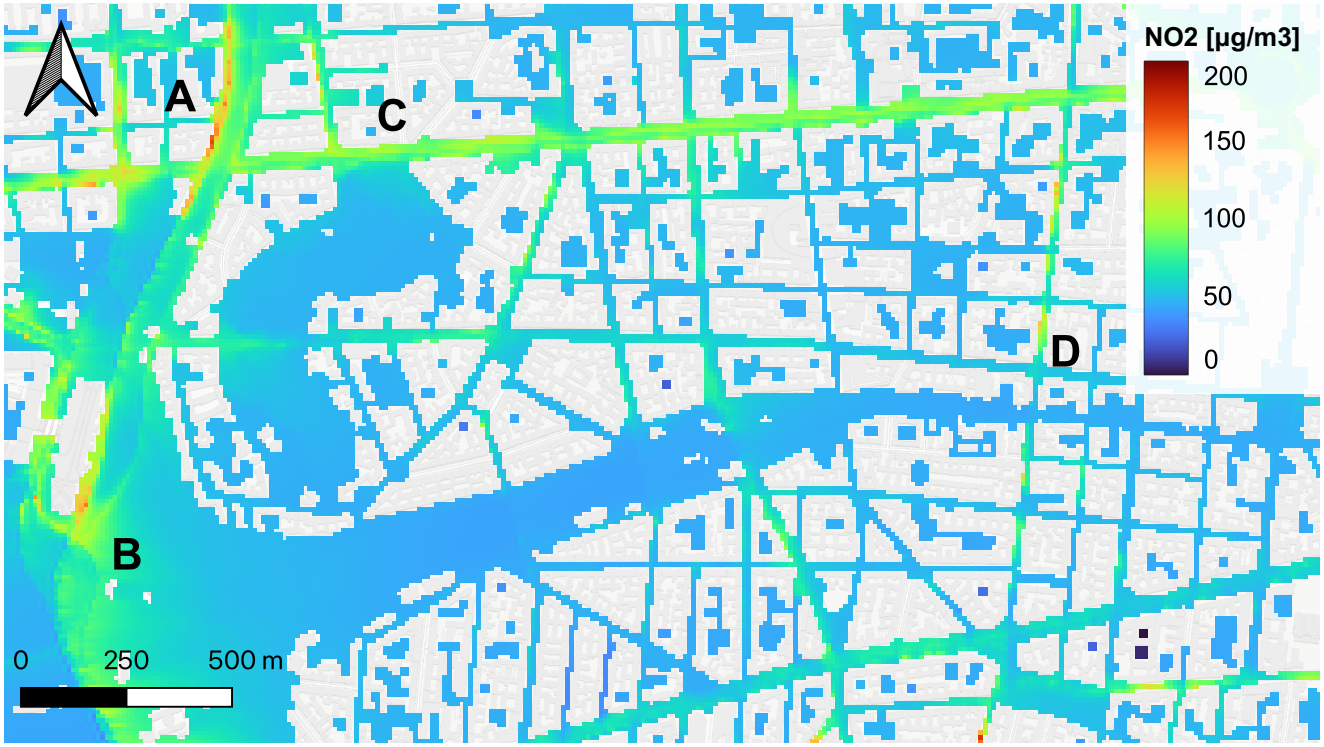

Figure 8. NO_2 concentrations on a continuous scale. The area depicted corresponds to the rectangle in Figure 7b. Effects of the building layout and the street layout are highlighted by letters A–D.

4. Application of Coupling Method

The capabilities of the developed coupling mechanism are demonstrated by conducting an idealized case study in Berlin, the capital of Germany. The primary aim of this study is threefold:

1. Demonstrate the functionality of the coupling mechanism by feeding traffic emission data into PALM-4U.
2. Evaluate the plausibility of the model outputs under idealized conditions, chosen to highlight potential high pollutant concentrations. Specifically, we test the system in low and steady wind conditions, where dispersion is minimal, expecting this setup to amplify pollutant concentration effects.
3. Investigate the ability of the coupling mechanism to detect air pollution *hot spots* in the urban area caused by traffic emissions. These findings provide the foundation for future studies involving more complex, real-world setups and validation.

To ensure the evaluation is focused on the coupling mechanism itself, we deliberately simplify real-world conditions by simulating traffic of a typical workday and by applying a constant wind speed of 1 m/s. This low wind speed was selected to limit atmospheric dispersion, creating a scenario where the influence of traffic emissions on air quality is most pronounced. Furthermore, the study is conducted for a summer day, a period when traffic emissions are expected to dominate due to the absence of residential heating.

Our focus in this study is on NO_x concentrations, given their significance for urban air quality and health impacts. While other pollutants such as CO, VOC (volatile organic compounds), and UHCs (Unburned Hydrocarbons) also have negative health effects, we prioritize NO_x because, together with particulate matter, it is one of the main contributors to air pollution-related health issues [4]. Additionally, NO_x is a reactive chemical species, and PALM-4U's ability to simulate chemical reactions allows us to evaluate the model's handling of the transport and transformation of such pollutants. Although CO_2 (Carbon Dioxide) is also emitted by traffic, it is a global greenhouse gas and not the focus of this study as we are concerned with the local dispersion and chemical behavior of pollutants that directly affect urban air quality.

The results of the idealized case study are evaluated with a focus on four points:

1. Comparison with measurement data;
2. Correlation with traffic volumes;
3. Investigation of additional factors such as wind direction, building and street layout, time of day, and potential artifacts;
4. Detection of emission hot spots.

The idealized case study is executed on a cluster of ten Intel Xeon Platinum 9242 processors, each offering 48 CPU cores. The wall-clock time for the presented PALM-4U setup is 52 h. The MATSim setup is run on the same computing platform, using only a single machine. The wall clock time for executing the traffic simulation is 12 h.

4.1. MATSim Setup Used for the Application

The Open Berlin Scenario [48,49] setup serves as the basis for calculating traffic emissions. It encompasses the city of Berlin (blue border in Figure 9), as well as a part of the surrounding state of Brandenburg. The traffic simulation setup includes 494,107 simulated people, which corresponds to a 10% sample of the population of Berlin and Brandenburg. To compensate for the sampled demand, Ziemke et al. [48] reduce the flow and storage capacities of the road network accordingly to achieve comparable traffic dynamics as if the entire population were represented in the simulation setup. Therefore, a single vehicle traveling on the simulated network represents ten vehicles in reality and emissions produced by a simulated vehicle must be multiplied by a factor of 10 to compensate for the sampling of the traffic demand. A detailed road network, generated from OSM data, including all road types from motorway to the residential level, is available within the city boundaries of Berlin, as shown in Figure 9. For the surrounding federal state of Brandenburg, a street network, including major and secondary roads, is used. The traffic simulation setup also includes a timetable-based public transportation system generated from a GTFS (General Transit Feed Specification) dataset available for Berlin and Brandenburg. The simulated people included in the traffic simulation setup can adjust their behavior by either switching modes of transport, selecting different routes within the same mode or adjusting the departure times of their trips.

As preparation for the presented study, a new network is generated from OSM data to provide detailed road geometries necessary for creating the chemistry driver file as described in Section 3.4. Additionally, the newly created network contains HBEFA road-type information based on the street types contained in OSM. Since the traffic simulation is conducted on a new road network which includes data to reconstruct detailed road geometries (see Section 3.1), all route information referencing the old network must be cleared from existing plans held by simulated people. To let the traffic simulation adapt to the new network, 100 iterations are performed until a new equilibrium as described in Section 2.1 is reached. To accelerate the process, simulated people are only allowed to adapt their behavior by adjusting routes, instead of also selecting different modes of transportation or adjusting departure times of their trips. Based on the newly created traffic simulation setup, traffic emissions are calculated, using the average vehicle fleet composition in Germany in 2020, as this data set closest to the date simulated with the PALM-4U setup. Road categories which are considered in the emission calculation are derived from free flow speeds found in the original OSM data. Subsequently, using the conversion method presented in Section 3, the chemistry driver file is created for the domain covered by the PALM-4U setup (Figure 9 red area). The temporal resolution of the emission flows in the chemistry driver are set to one hour, as this was the only available temporal resolution option at the time the study was conducted. Figure 7a shows the result of the NO_2 emission calculations and the subsequent conversion for the period between 8 and 9 am.

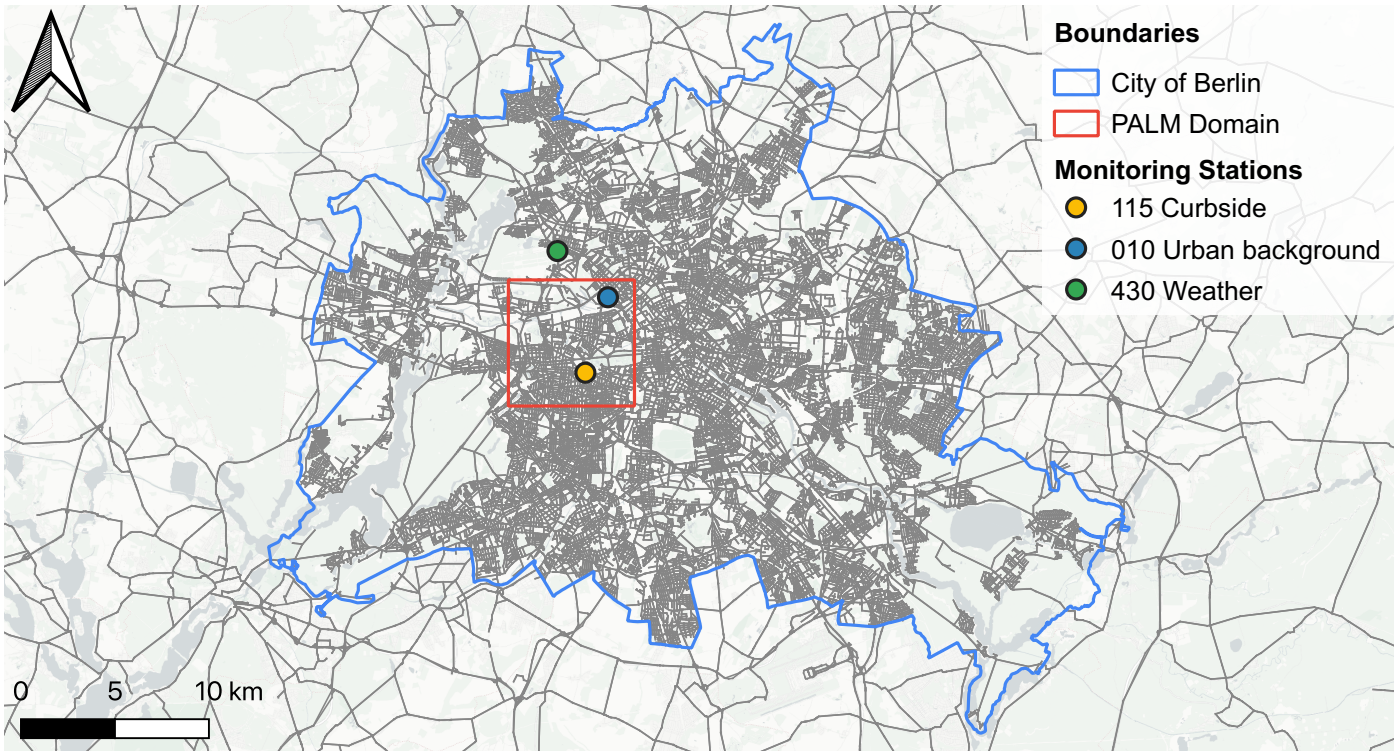

Figure 9. The city boundaries of Berlin (blue), as well as the PALM-4U-Domain boundaries (red). Within the city boundaries, a detailed road network (gray) is included. For the remaining MATSim domain, only major roads are included. The MATSim traffic simulation setup stretches beyond the depicted area.

4.2. PALM-4U Setup Used for the Application

For the dispersion calculation, the PALM Berlin model created by [30,50] is used and supplemented. The covered model area is shown in red in Figure 9. It includes a square area with a side length of 6.71 km and extends 3.6 km vertically. The grid has a resolution of 10 m in the horizontal and vertical direction. Above the height of 2.7 km, the resolution gradually becomes coarser in vertical direction. The model also includes road types, building heights, water bodies, soil conditions, and vegetation. The simulation is configured for 17 July 2017, chosen as a "typical Berlin" summer day with temperatures between 16 and 25 °C, scattered clouds, and predominantly westerly winds. For traffic emissions, the original setup uses the parameterized LOD 0 emission mode, where traffic emissions are based on road types and a simplified diurnal profile. Cyclic boundary conditions are used at the lateral boundaries of the model domain, asserting a continuous in and outflow of pollutants. According to Khan et al. [30], this is a reasonable approach as the simulation domain is situated within a large urban area.

This setup is adjusted to run in LOD 2 mode, in which input emissions for the PALM-4U simulation are provided by a chemistry driver file. Instead of using parameterized traffic emissions, the adjusted PALM-4U model setup uses emissions generated with the MATSim traffic model, which were transformed into the PALM-4U chemistry driver format using the methodology described in Section 3. Four species, NO, NO_2, particulate matter, and O_3 (Ozone), are simulated, using the photo stationary state mechanism for the gas-phase chemistry. Additionally, dynamic wind speeds and wind directions are deliberately simplified to a steady wind flow of 1 m/s from a western direction. This simplification replaces the realistic variations in wind conditions throughout the day with constant values, providing a controlled environment to explore the specific effects of traffic emissions on dispersion patterns. To provide sufficient spin-up time, two consecutive days are simulated using the same 24 h traffic emissions. The following analysis is conducted using only data from the second day, which corresponds to the 17 July 2017, as in the original model set up.

4.3. Simulation Results

For the conducted PALM-4U simulation, averaged masked output files are produced. The averaging interval is set to one hour, matching the temporal resolution of the input traffic emissions. The mask follows the terrain structure, allowing the analysis of the bottom layer above ground, which extends up to a height of 10 m. We focus on the bottom layer of the masked output because this is the layer into which road traffic emits emissions. Figure 7b shows averaged NO_2 output concentrations of the conducted PALM-4U run for the time between 8 and 9 am for the covered model area.

4.3.1. Comparison with Measurement Data

To assess the plausibility of the simulated air pollution concentrations, a comparison is conducted between simulated and observed NO_x concentrations. The simulation domain of the PALM-4U setup encompasses two monitoring stations: one curbside and one urban-background station [51]. The comparison focuses on the urban-background monitoring station 010, located in the northern part of the PALM-4U simulation domain. Curbside station 115 is influenced significantly by frequent diesel bus traffic due to its proximity to a major city bus hub and is excluded from this comparison [52].

Figure 10 presents a comparison of simulated NO_x concentrations with monitoring data at the urban-background station 010, along the emission inflow caused by the closest link. In the plot, hourly average concentration values from the simulation, at the monitoring station, are depicted in red, hourly concentration values from the monitoring station on different days are shown in varying shades of blue, and the flow of traffic emissions into the PALM simulation caused by the closest link is shown in yellow.

The simulation setup represents an artificial summer day, incorporating traffic volumes typical for a workday and constant low wind conditions of 1 m/s from the western direction. To ensure a suitable basis for comparison, we select measured data from June, July, and August, specifically choosing the five days with the lowest average wind speeds. Average wind speeds measured at weather monitoring station 430 Tegel [53] during these selected days range from 1.3 m/s to 1.7 m/s, with lower speeds (between 0 m/s and 2 m/s) in the morning hours (midnight to 8 am) and higher speeds (between 1 m/s and 3 m/s) from 8 am to 6 pm. Wind speeds during the remaining evening hours are similar to those in the morning. Although monitored concentrations also include emissions from sources such as residential heating, manufacturing, and energy supply, we assume that the measurement data are predominantly influenced by road traffic. Residential heating does not play a significant role during summer, and emissions from road traffic are in closer proximity compared to sources like manufacturing or energy supply [4].

Examining Figure 10, simulated NO_x concentration levels hover around 50 $\mu g/m^3$ from midnight to 4 am, followed by an increase between 4 am and 9 am, peaking at 103 $\mu g/m^3$ at 6 am. From 9 am to 8 pm, NO_x concentrations decrease from 47 $\mu g/m^3$ to 23 $\mu g/m^3$ before rising again during the subsequent simulated hours. Analysis of the monitoring data reveals a varied picture during the early night hours (1 am to 4 am), with three days exhibiting relatively low concentration values (13 $\mu g/m^3$ to 40 $\mu g/m^3$) and two days showing notably higher values (up to 105 $\mu g/m^3$). On all selected days, a concentration peak is observed in the morning hours between 8 am and 9 am, except for one day with a peak at 7 am. Between 9 am and 8 pm, NO_x concentrations decline on all selected days before increasing again during the later hours.

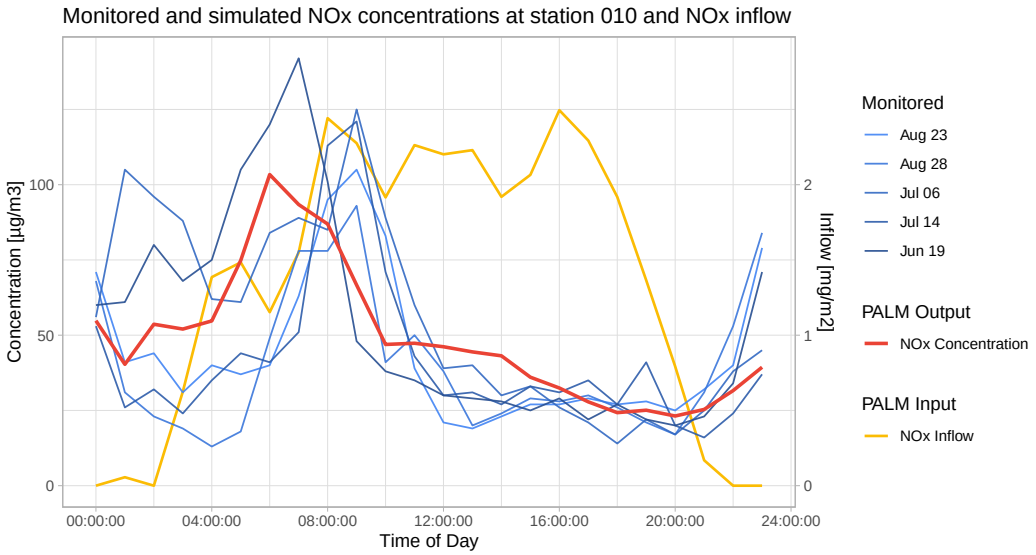

Figure 10. Comparison of simulated and monitored NO_x concentrations at urban background monitoring station 010. Simulated hourly averages of NO_x concentration values are depicted in red. Hourly averages of monitored NO_x concentration values at urban background station 010 for days with low wind speeds in blue tones. The emission inflow from the closest link is depicted in yellow. One clearly sees that the PALM output (red) is not just a rescaled version of its input (yellow) but that there are quite strong non-linear processes at work.

Comparing simulated, and measured concentration levels reveals a similar daily pattern. Early night and morning hours exhibit relatively low concentration values, followed by a morning peak. Concentrations during the remaining daylight hours remain relatively low before rising during late-night hours. The NO_x concentrations present in the early morning hours even though almost no input emission flows are present are caused by pollution being emitted during the warm-up phase of the simulation. Simulated NO_x concentrations align within the range of measured values for respective hours of the day, except for the period between noon and 4 pm. During these hours, wind speeds at weather monitoring station 430 were higher than 1 m/s on all selected days, which might have led to a higher rate of dispersion compared to the simulation. Notably, the peak in concentration values for the simulated data occurs earlier than for the measured data. This observation suggests a reduced presence of turbulence in the model during the early morning hours when the boundary layer remains stable, contrasting with real-world conditions. In the model, turbulence is primarily generated by wind and radiation, while in reality, additional factors such as turbulence induced by moving vehicles may contribute to a greater dispersion of pollutants, surpassing what can be observed in the current model setup.

The emission inflow curve in Figure 10 reveals a distinct pattern compared to the concentration data. The inflow of traffic emissions into the PALM simulation increases sharply in the early morning hours, reaching a peak of 2.44 mg/m^2 at 8 am, and remains relatively high throughout the day, before gradually decreasing towards 0 in the evening. Despite this sustained high inflow, the simulated NO_x concentrations exhibit a morning peak, followed by relatively low values for the remainder of the day.

This comparison demonstrates that the simulated NO_x concentrations, while being distinct from the pattern of traffic emission inflow, closely follow the observed monitoring data throughout the day. The PALM simulation effectively transforms the inflow of traffic emissions into concentration levels that align with the measured data, particularly capturing the morning peak and subsequent decrease. This indicates that the PALM-4U model accurately disperses traffic emissions over the course of the day, resulting in realistic NO_x concentration patterns that match real-world observations.

4.3.2. Traffic Volumes

Investigating Figure 7b shows that the overall pattern of NO_x concentrations represents the pattern of input emissions from the chemistry driver file in Figure 7a. Street segments with high traffic volumes and high emission flows produce higher pollutant concentrations within their vicinity. Major roads like the inner-city motorway on the left and arterial roads are clearly recognizable. The areas with the highest pollutant concentrations are located close to the inner-city motorway near the western edge of the model domain. Pollutant concentrations range between 150 $\mu g/m^3$ and 200 $\mu g/m^3$ in obstructed areas and 80 $\mu g/m^3$ to 100 $\mu g/m^3$ in unobstructed ares. For residential roads, concentration values between 50 $\mu g/m^3$ and 80 $\mu g/m^3$ can be observed, depending on their situation relative to the wind direction. Areas far away from road traffic show concentration values up to 50 $\mu g/m^3$.

Though the overall pattern of pollutant concentrations in Figure 7b is dominated by traffic volumes, investigating concentration levels in more detail reveals other factors which have a high influence on concentration levels:

- Wind direction;
- Building and street layout;
- Time of day;
- Raster and simulation artifacts.

4.3.3. Wind Direction

Wind direction has a major influence on concentration levels observed in the PALM-4U output data. In the area surrounding point A in Figure 7b, high pollutant concentrations between 75 $\mu g/m^3$ and 200 $\mu g/m^3$ are noticeable along the inner-city motorway, running in a north–south direction. Since the motorway is not obstructed by buildings in that area, the traffic emissions are transported with the wind direction and gradually dissipate. A similar effect can be observed for the area around B, which contains several arterial roads leading through Berlin's largest park. Emitted pollutants dissipate evenly on both sides of the street, which is parallel to the general wind direction, and dissipate with the wind for the street perpendicular to this direction. Notably, obstructed roads exhibit distinct dispersion patterns, as detailed in Section 4.3.4.

4.3.4. Building and Street Layout

The layout of buildings surrounding street corridors influences the simulated pollutant concentration levels. The areas around A, B, and C in Figure 8 represent distinct layout situations and their influence on pollutant concentration levels. The color ramp in Figure 8 is capped at 200 $\mu g/m^3$, effectively excluding 0.04% of outliers (see Section 4.3.6) in the 8 am time period and reveals concentration patterns on a smaller scale.

The effects of the building layout interact with the general wind direction as can be seen when investigating concentrations close to the city motorway near A and B in Figure 8. Both motorway sections have comparable traffic volumes but show different concentration levels. The motorway section around B has almost no buildings in the vicinity, which lets air flow over the motorway without obstructions. Traffic emissions are taken up from the street level and transported with the wind direction while being diluted in the process. Concentration levels near unobstructed motorway sections near B reach 75 $\mu g/m^3$ to 100 $\mu g/m^3$. In contrast, near A, both sides of the motorway are obstructed by relatively high buildings forming a street canyon. Within that street canyon pollutant concentrations are generally higher compared to the area around B with concentration levels ranging between 80 $\mu g/m^3$ and 150 $\mu g/m^3$. As the motorway section is situated in a street canyon topology, traffic emissions cannot be transported freely with the wind direction but are retained within the street canyon. Within the street canyon, the highest concentration levels up to 150 $\mu g/m^3$ can be observed near buildings located on the upwind side of the motorway. This effect is caused by eddies forming behind obstacles that obstruct the wind flow. While the air flow at the roof level follows the general wind direction, the eddy caused by the obstructing building reverses the wind direction at street level. The traffic

emissions emitted by vehicles traveling on the motorway are therefore transported against the general wind direction towards the buildings on the western side of the motorway leading to high pollutant concentrations there.

Another effect of building layout can be observed in area C in Figure 8 where we have comparable pollutant concentrations to the downwind side of the motorway in area A. Due to the building layout along the street, a narrow street canyon is formed from which traffic emissions cannot dissipate, leading to high concentration levels with values ranging from 80 $\mu g/m^3$ to 120 $\mu g/m^3$ even though traffic volumes on the arterial road are only roughly half of what can be observed on the city motorway.

In addition to the building layout, pollutant concentrations are influenced by the street layout relative to the overall wind direction. The area around D in Figure 8 shows NO_2 concentrations for the intersection of Kantstrasse/Leibnitzstrasse, of which both streets have comparable traffic volumes. Still, the street perpendicular to the overall wind direction shows higher pollutant concentrations of up to 120 $\mu g/m^3$ due to the street canyon effect (described above), which captures traffic-induced pollutants within said street canyon. For the street parallel to the overall wind direction, emissions are transported along the street corridor and eventually dissipate, leading to much lower concentration levels between 55 $\mu g/m^3$ and 70 $\mu g/m^3$.

Additionally, elevated pollutant concentrations are observed in shaded areas, contrasting with lower concentrations in sun-exposed regions. This distinction arises from the temperature variation between shaded and sunlit areas, where the latter experience higher temperatures due to direct sun radiation. The temperature discrepancy influences the vertical motion of air, with colder areas exhibiting reduced upward transport compared to warmer regions. This diminished vertical transport results in higher pollutant concentrations in colder, shaded areas. Additionally, for NO_2, an additional factor comes into play where, in the absence of sunlight, the photochemical reaction required for breaking down NO_2 into NO and O_3 does not take place. Consequently, NO_2 persists in the atmosphere, contributing to higher NO_2 concentrations in shaded areas. Both effects are also described in the analysis of the original PALM-4U setup provided by Khan et al. [30].

4.3.5. Time of Day

Figure 10 shows simulated NO_x concentration levels in comparison to the measurements of urban background monitoring station 010. Examining the output concentration levels of the PALM-4U setup depicted in red reveals a high fluctuation during different hours of the day with a peak for NO_x concentrations between 6 and 8 am (see Section 4.3.1). During that time period of the day, the morning traffic rush hour has already started, while the atmospheric boundary layer is still relatively shallow and upward transport by convection has not yet fully started. The remainder of the day shows much lower NO_x concentrations on the ground levels as upward transport and photochemical reactions reduce concentration levels in the bottom layer of the atmospheric model. This process is also described in the model analysis presented by Khan et al. [30].

The temporal variation in pollutant concentration appears significantly more pronounced than the spatial variation within a given time period. The comparison between simulated and observed NO_x concentrations highlights that, despite the distinct pattern of traffic emission inflow, the PALM simulation effectively disperses and dilutes the emissions, resulting in concentration levels that closely align with the monitoring data. For example, the simulated concentration levels from Figure 10 reveal a notable fluctuation in NO_x concentrations, with a factor of 4.5 difference ranging from 23.1 $\mu g/m^3$ at 8 pm to 103.3 $\mu g/m^3$ at 6 am. In comparison, the simulated NO_x concentrations for all grid points between 7 and 8 am show a much narrower range, varying only between 81.4 $\mu g/m^3$ and 95.0 $\mu g/m^3$ for the 50% values closest to the median value over the model domain (excluding outliers exceeding 200 $\mu g/m^3$). This observation suggests that the primary influence on concentration levels is the time of day, attributed to the upward transport of pollutants and the occurrence of photochemical reactions.

4.3.6. Artifacts

The distribution of concentration levels shows a very long tail of higher than average concentration levels for the individual time periods. The majority of simulated concentration values lie within a small range below 100 $\mu g/m^3$, as described in Section 4.3.5, while maximum concentration levels reach up to 2000 $\mu g/m^3$. Investigating raster cells with concentration levels higher than 200 $\mu g/m^3$ (representing 0.016% of all values) reveals different patterns of outliers, sorted from most to least severe:

1. **Raster Artifacts:** The highest concentration levels can be observed due to artifacts as a result of the rasterization process. The leftmost map in Figure 11 gives an example of such a case: The underlying street has a relatively high traffic volume, while the rasterization algorithm to generate the static driver of the PALM-4U model decided that tiles covered by the street are in the simulation covered by buildings. The emissions produced with MATSim are then distributed onto the remaining raster tiles covering that link. This leads to very high concentrations in the first place because emissions that were emitted over the entire length of the link are mapped onto a smaller number of raster cells than what the length of the link would suggest. Additionally, in this particular case the wind direction blows emissions into an artificial dead end at the end of the street corridor, leading exceedingly high simulated concentrations of up to 2000 $\mu g/m^3$.
2. **Resolution and Grid Layout:** Due to the relatively coarse resolution of 10m, streets lying in narrow street canyons are sometimes represented by only a single pixel row. The map in the center of Figure 11 demonstrates this issue, where a street with moderate traffic volumes causes exceedingly high pollutant concentrations of up to 600 $\mu g/m^3$. The angle at which the street canyon is situated compared to the grid structure forms multiple caverns where turbulence does not formcorrectly and pollutants are not transported away from the ground level.
3. **Stacked Streets:** The rightmost map in Figure 11 shows another special case where exceedingly high pollutant concentrations can be observed. In the case depicted, the model has two stacked street levels. The lower one is a six-lane motorway, while the upper one is a four-lane arterial road. As the implemented mechanism does not resolve emission flows in vertical direction but assumes all emissions to emerge from ground level, the emissions of both streets are emitted into the same raster tile, leading to high pollutant concentrations between 200 $\mu g/m^3$ and 400 $\mu g/m^3$.
4. **Numerical effects:** The applied raster method distributes emissions from one link onto a single line of raster cells, leading to high emission flows in those cells. In contrast, adjacent raster cells, which might also be covered by a street show no emission flows. The large difference of emission flows in adjacent raster cells leads to numerical effects in the CFD model causing less pronounced dispersion of traffic emissions.

Mitigating the listed types of artifacts could be accomplished with different strategies. The most straightforward improvement would be to increase the resolution of the simulated setup, which would solve item (2) at the cost of higher computational demands. For the mitigation of numerical effects, item (4), the raster algorithm must be switched to an algorithm which accounts for the width of the simulated street, distributing the rastered emissions on a line which is wider than a single pixel. This improvement would also require a higher resolution of the model grid to achieve a substantial improvement. Avoiding concentration outliers due to raster artifacts, item (1), could be accomplished by applying a pre-processing before the PALM-4U simulation starts, where raster cells that are labeled as buildings but for which the chemistry driver provides traffic emissions could be relabeled as streets in the static driver file. Modeling stacked streets, item (3), correctly is not trivial and would require changes in both models. The traffic model would have to have information on the vertical layout of streets, while the chemistry driver would have to provide the ability to place traffic emission sources in vertical direction. Modeling stacked structures

like bridges correctly would also require a higher resolution of the simulation setup at the expense of increased computational costs.

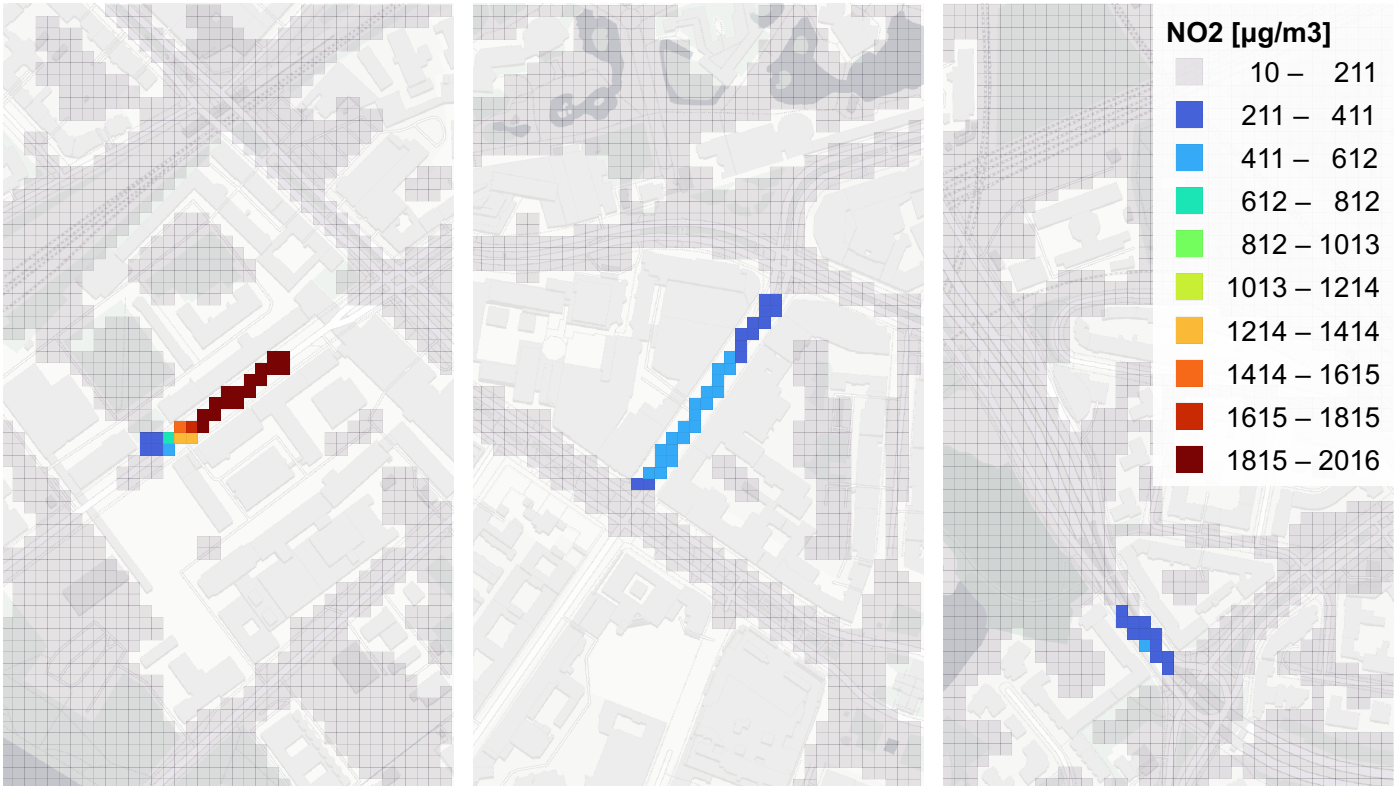

Figure 11. NO_2 concentrations for the time period between 8 am and 9 am, showing areas with exceptionally high pollutant concentrations due to artifacts in the simulation setup. The coloring uses equal intervals to highlight outliers on the long tale of the concentration value distribution.

4.3.7. Detecting Pollutant Concentration Emission Hot Spots

The simulation results of the coupled traffic emission and dispersion models allow the detection of traffic induced pollution hot spots. These are the areas which are significantly impacted by traffic emissions. Pollution hot spots can be defined in multiple ways, the most common one being ambient threshold concentration values which must not be exceeded within a certain time period.

EU regulations define a annual mean limit value of 40 µg/m^3 for NO_2, as well as an hourly limit value of 200 µg/m^3, which must not be exceeded by more than 18 h per year [4]. The monitoring of these threshold values is conducted with curbside monitoring stations. For the simulated domain, two air quality monitoring stations are situated in the simulation domain as shown in Figure 12a. Compared to the point-based monitoring, the introduced mechanism allows for a comprehensive investigation of threshold violations within the simulated domain. Figure 12a shows threshold violations for an arbitrary threshold of 80 µg/m^3, which was selected to receive a spatially differentiated image for the time period between 8 and 9 am. The image shows that large parts of the motorway, as well as most of the major roads, cause concentrations above the chosen threshold value, especially when situated within a street canyon perpendicular to the wind direction. Figure 12a also shows that both monitoring stations are not affected by the threshold violations, indicating that their position does not correspond to where the highest pollutant concentrations are to be expected, at least for the simulated west wind weather conditions.

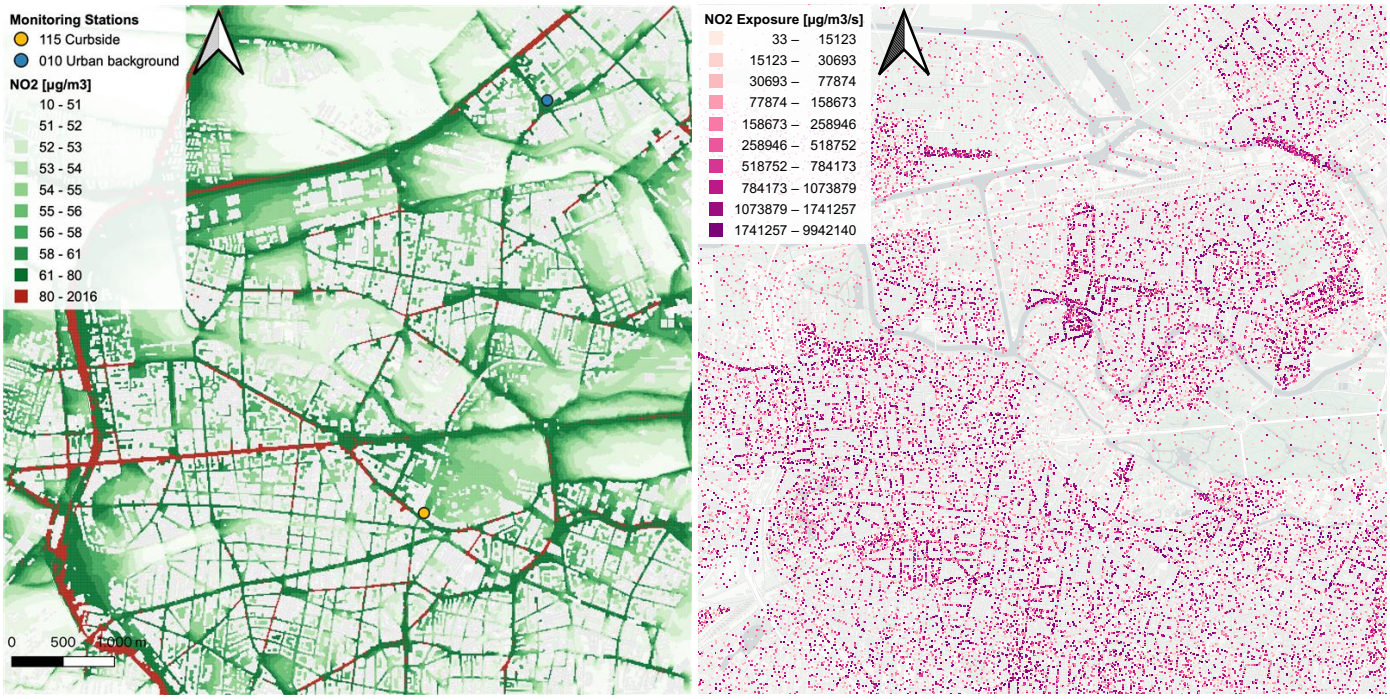

(**a**) (**b**)

Figure 12. Two methods to identify emission hot spots: (**a**) uses a threshold approach showing NO_2 concentrations below and above 80 µg/m^3 and two curbside monitoring stations. (**b**) shows exposure to traffic emissions at activity locations.

As health effects due to pollution do not correspond to threshold values, another possible way of mitigating health effects is to limit a population's exposure to such pollutants. The Open Berlin Scenario setup, used for our idealized case study, incorporates calibrated activity locations and times, as described by Ziemke et al. [48]. With access to activity locations and times in MATSim, it is straightforward to calculate an exposure index for raster tiles of a simulated PALM-4U domain. Activities which are situated within raster tiles marked as buildings are mapped onto the closest outside raster tile. The observed concentration value c_p is then multiplied with the time t_a spent within this raster tile at the given concentration, as shown in Equation (1):

$$E = t_a \times c_p \tag{1}$$

Applying this method to the simulation domain yields Figure 12b, which indicates that exposure hot spots are not necessarily situated where the highest pollutant concentrations can be observed. The northwest part of the inner-city motorway, where high pollutant concentrations can be observed, does not pose a large problem when evaluating traffic emissions by exposure impact as this stretch of the motorway is situated in an area with low activity density. In comparison, other areas with lower absolute pollutant concentrations cause much higher exposure to traffic emissions due to higher density of activities. The proposed exposure analysis only considers time spent at activities and does not account for exposure to pollution during trips.

5. Discussion

This section provides a detailed comparison of our findings with previous studies and discusses the impact of different modeling approaches, particularly the use of LES vs. RANS and the importance of accurately simulating traffic emissions.

5.1. Comparison with Other Studies

Our study shares similarities with the works of San José et al. [38] and Sanchez et al. [37], both of which model traffic emissions using CFD models. However, key methodological differences set our approach apart.

San José et al. [38] use SUMO (Simulation of Urban MObility) [54] as their traffic model, the EMEP/EEA Air Pollution Emission Inventory Guidebook [55] to generate emissions from traffic, and MICROSYS (a CFD model for urban air quality) [56] as meteorological model. SUMO, similar to MATSim, follows individual vehicles, but different from MATSim, computes values for acceleration and braking. However, the EMEP/EEA approach uses HBEFA, i.e., the same data that we use, as their sub-model for traffic, and in consequence, the end result is quite similar to ours in the sense that acceleration and braking are ignored and instead average emissions values are looked up based on traffic and road conditions. MICROSYS is a CFD-RANS model and thus steady state, in contrast to the PALM model system which we operate in LES mode. Traffic demand in San José et al. [38] is generated from counting stations, which is possible because the study considers a relatively small area. Thus, our study is quite similar to theirs, with the following important differences:

- In our work, the traffic demand is driven by a regional behavioral model. This allows, in future studies, to investigate behavioral responses to possible traffic demand management measures, which might be considered in order to improve air quality.
- The area covered by the domain used for the PALM-4U simulation is much larger than what was used in the study conducted by San José et al. [38]. Covering larger parts of the city is important to derive traffic management policies and their evaluation.
- In our work, a fully dynamic meteorological model is used, which we consider a more appropriate approach to the complex topologies of urban situations.

The second study, conducted by Sanchez et al. [37], uses VISSIM as their traffic model and TNO ENVIVER based on VERSIT+ micro [57] to generate emissions from traffic. Their meteorological model appears to be a unique RANS model. VISSIM, similar to SUMO, follows individual vehicles with acceleration and braking. The VERSIT+ micro approach, while bearing similarities to HBEFA in its use of lookup tables based on traffic and road conditions, is a distinct development by the Netherlands Organization for Applied Scientific Research independent of HBEFA. The publication does not specify the generation of the traffic demand and focuses on the investigation of one complex intersection. In consequence, the study presented by Sanchez et al. operates on a smaller (more detailed) scale. Other differences to our approach are similar to those given for San José et al. [38] in the paragraphs above.

Finally, Samad et al. (2024) demonstrate the sensitivity of PALM-4U to traffic management policies in Stuttgart, Germany. While they use PALM-4U, they do not generate emissions from a full traffic model; instead, they use a similar approach to the LOD 1 mode for emissions estimation described in Section 2.3. This limits the granularity and realism of their emissions data compared to our more detailed emissions modeling based on MATSim.

5.2. Pollutant Concentrations near Traffic Volumes

Our results show that traffic emissions are highest near roads with heavy traffic volumes, as indicated in Figure 7b and discussed in Section 4.3.2. This is consistent with findings from Samad et al. [58], who also observe elevated pollutant concentrations near busy roads. Similarly, Sanchez et al. [37] report that the highest NO_x concentrations occur near roads with high traffic volumes during peak hours. San José et al. [38], despite focusing on a smaller area, also find pollutant peaks in close proximity to traffic.

5.3. Temporal Variations in Pollutant Concentrations

Our model accurately captures the morning peak in NO_x concentrations, as shown in Figure 10 and discussed in Section 4.3.1. This aligns with San José et al. [38], whose RANS-based CFD model also reflects daily traffic peaks. However, Sanchez et al. [37] note that their model overestimates NO_x concentrations compared to measurements, attributing this to the neglect of thermal effects. In contrast, Samad et al. [58] find that their PALM-4U simulation underestimates NO_x concentrations compared to measurement stations, speculating that the emission input data might be responsible for this discrepancy. Interestingly, Samad et al. assume that all diesel vehicles adhere to the Euro 4 standard, a worst-case scenario, which should lead to an overestimation in concentration values rather than an underestimation.

5.4. Wind Direction and Urban Geometry

The results indicate that emission dispersion works well regarding wind direction and building and street layout, as described in Sections 4.3.3 and 4.3.4. Our findings are consistent with those of the other three studies. The most interesting comparison is with San José et al. [38]. Similar to our findings, their model results show that traffic emissions are transported along street canyons that are parallel to the overall wind direction. In the case of unobstructed areas, their model results show that emissions are freely dispersed into the direction of the wind, which is similar to our findings.

For street canyons that are perpendicular to the wind direction, the situation differs. As described in Section 4.3.4, our model results show maximum concentrations on the upwind side of buildings, caused by eddies forming within the street canyon. In contrast, the results from San José et al. [38] indicate that maximum concentrations in similar street canyons occur on the downwind side. This difference may be attributed to the different CFD models used: the RANS model employed by San José et al. [38] parameterizes turbulence, while the LES model used in our study resolves a significant portion of the turbulent structures.

The location of maximum concentrations on the upwind side of street canyons is consistent with what we would expect, as described by Maronga et al. [46], Chew et al. [59], Zheng and Yang [60], who also highlight that LES models are more capable of capturing these phenomena. However, using an LES model instead of a RANS model comes at a significantly higher computational cost—up to 50 times greater, as stated by Zheng and Yang [60].

5.5. Spatial Resolution and Model Area

Spatial resolution significantly impacts the accuracy of pollutant dispersion modeling in urban environments. In this study, we use a 10-meter grid, whereas Sanchez et al. [37] and San José et al. [38] employ finer grid resolutions of around 5 m. The finer grids used in those studies offer more detailed insights, especially for localized areas, and help avoid issues like rasterization artifacts and closed streets—issues we observed with our coarser grid.

While our 10 m resolution introduces limitations in capturing small-scale variations, particularly in dense urban canyons, the larger model domain allows us to investigate emission hot spots across a broader urban area. As demonstrated in Section 4.3.7, this approach enables us to analyze both violations of emission thresholds and exposure to traffic emissions on a citywide scale. With the smaller domains used by San José et al. [38] and Sanchez et al. [37], comparable investigations are limited to localized areas.

6. Conclusions and Outlook

This study presents the successful coupling of MATSim with PALM-4U to simulate traffic emissions and dispersion across large urban areas. Key advantages of coupling both models include:

1. **Large model domain:** The strength of the presented coupling lies in its ability to model large-scale urban environments. MATSim is specifically designed to simulate traffic patterns over extensive urban areas, and PALM-4U is well suited for large HPC

systems. Together, they enable the accurate simulation of air pollution concentrations across large city districts, providing insights that are critical for citywide air quality management.

2. **High-accuracy dispersion:** While other studies have used finer grid resolutions (e.g., 5 m), our results demonstrate that a 10-meter grid is sufficient to identify emission and exposure hot spots. Though this coarser resolution introduces challenges like raster artifacts, it effectively captures concentration patterns caused by road traffic. Using a LES model provides advantages compared to RANS models, as turbulence forming in street canyons, wider than the grid resolution, is simulated accurately. Additionally, PALM-4U's ability to simulate chemical reactions and boundary layer effects yields good agreement between simulated and measured NO_x concentrations. When even higher precision is required, the coupling methodology can easily support the use of finer grid resolutions in future studies.
3. **Behavioral traffic model:** A unique advantage of our approach lies in the behavior-based traffic model of MATSim, which operates at the mesoscale and is sensitive to changes in traffic management policies. Due to its agent-based nature, individual behavioral responses to policy interventions can be simulated. Future research can leverage this capability to test various traffic management strategies and their impact on air pollution.

Finally, as both MATSim and PALM-4U are open source, this framework is readily accessible for adaptation and further development by the broader scientific community, promoting reproducibility and collaborative improvement.

Building on the results of this study, several areas of future work are planned to further improve the accuracy and applicability of the coupled MATSim and PALM-4U model system:

- **Real-world case study**: A next step is to conduct a real-world case study under realistic meteorological conditions. This simulation will allow for direct comparison with measured data from air quality monitoring campaigns, providing validation and fine-tuning of the model's performance in real urban environments.
- **Traffic management policy evaluation**: A study investigating traffic management policies is currently in progress. This will enable us to simulate various traffic interventions aimed at mitigating pollution hot spots. The traffic model in MATSim can simulate the behavioral responses to these policies, producing new traffic patterns and emissions data. These emissions will then be used as inputs for PALM-4U, and the resulting pollution dispersion patterns will be analyzed to assess the effectiveness of different policy measures.
- **Improving the coupling methodology**: There are opportunities to further enhance the coupling between MATSim and PALM-4U. MATSim can compute x, y coordinates with a one-second resolution for all vehicles, offering the potential to calculate emissions based on these detailed trajectories. Feeding this high-resolution traffic emission data into PALM-4U would provide even more accurate simulations of urban air pollution. Work on this improvement is currently underway.

Author Contributions: Conceptualization, J.L., S.B. and K.N.; data curation, J.L.; formal analysis, J.L., S.B. and K.N.; investigation, J.L. and B.K.; methodology, J.L. and S.B.; project administration, S.B. and K.N.; resources, B.K.; software, J.L.; supervision, S.B., B.K. and K.N.; validation, J.L., S.B. and B.K.; visualization, J.L.; writing—original draft, J.L.; writing—review and editing, S.B., B.K. and K.N. All authors have read and agreed to the published version of the manuscript.

Funding: This work was partially funded by the BMBF—Bundesministerium für Bildung und Forschung grant number 01LP1911C.

Institutional Review Board Statement: Not applicable.

Informed Consent Statement: Not applicable.

Data Availability Statement: The conversion tool described in this article can be found at https://gitlab.palm-model.org/matsim/matsim_traffic_emmisions/-/tree/mosaik-2-01 (accessed on 28 August 2024), an open-source git repository hosted as part of the PALM model system and was run with the version captured in [61]. The MATSim setup can be found at https://github.com/matsim-scenarios/matsim-berlin/releases/tag/mosaik-2-01 (accessed on 28 August 2024) and was run with the *MosaikRunner.java* class [49]. The original PALM-4U setup can be found at 10.5281/zenodo.4153388, a data repository stored at the Zenodo project [50]. All input and output data related to this article can be found at https://doi.org/10.14279/depositonce-18737 (accessed on 28 August 2024), a data repository hosted at Technische Universität Berlin [62].

Acknowledgments: The authors gratefully acknowledge the computing time made available to them on the high-performance computer "Lise" at the NHR Center NHR@ZIB. This center is jointly supported by the Federal Ministry of Education and Research and the state governments participating in the NHR (www.nhr-verein.de/unsere-partner (accessed on 28 August 2024)).

Conflicts of Interest: The authors declare no conflicts of interest.

References

1. Desa, U.N. *World Urbanization Prospects 2018: Highlights*; Technical Report; United Nations: New York, NY, USA, 2018.
2. Schulz, H.; Karrasch, S.; Bölke, G.; Cyrys, J.; Hornberg, C.; Pickford, R.; Schneider, A.; Witt, C.; Hoffmann, B. *Atmen*; DGfPuB eV; Deutsche Gesellschaft für Pneumologie und Beatmungsmedizin e.V.: Berlin, Germnay, 2018.
3. Ciarelli, G.; Colette, A.; Schucht, S.; Beekmann, M.; Andersson, C.; Manders-Groot, A.; Mircea, M.; Tsyro, S.; Fagerli, H.; Ortiz, A.G.; et al. Long-term health impact assessment of total PM2.5 in Europe during the 1990–2015 period. *Atmos. Environ. X* **2019**, *3*, 100032. [CrossRef]
4. European Environment Agency. *Air Quality in Europe: 2020 Report*; Publications Office of the European Union: Luxembourg, 2020.
5. Dons, E.; Int Panis, L.; Van Poppel, M.; Theunis, J.; Willems, H.; Torfs, R.; Wets, G. Impact of time–activity patterns on personal exposure to black carbon. *Atmos. Environ.* **2011**, *45*, 3594–3602. [CrossRef]
6. Lim, S.; Holliday, L.; Barratt, B.; Griffiths, C.J.; Mudway, I.S. Assessing the exposure and hazard of diesel exhaust in professional drivers: A review of the current state of knowledge. *Air Qual. Atmos. Health* **2021**, *14*, 1681–1695. [CrossRef]
7. McConnell, R.; Islam, T.; Shankardass, K.; Jerrett, M.; Lurmann, F.; Gilliland, F.; Gauderman, J.; Avol, E.; Künzli, N.; Yao, L.; et al. Childhood incident asthma and traffic-related air pollution at home and school. *Environ. Health Perspect.* **2010**, *118*, 1021–1026. [CrossRef]
8. Ehrnsperger, L.; Klemm, O. Air pollution in an urban street canyon: Novel insights from highly resolved traffic information and meteorology. *Atmos. Environ. X* **2022**, *13*, 100151. [CrossRef]
9. von Schneidemesser, E.; Sibiya, B.; Caseiro, A.; Butler, T.; Lawrence, M.G.; Leitao, J.; Lupascu, A.; Salvador, P. Learning from the COVID-19 lockdown in berlin: Observations and modelling to support understanding policies to reduce NO_2. *Atmos Env. X* **2021**, *12*, 100122. [CrossRef]
10. Gürbüz, H.; Şöhret, Y.; Ekici, S. Evaluating effects of the COVID-19 pandemic period on energy consumption and enviro-economic indicators of Turkish road transportation. *Energy Sources Recovery Util. Environ. Eff.* **2021**, 1–13. [CrossRef]
11. Forehead, H.; Huynh, N. Review of modelling air pollution from traffic at street-level—The state of the science. *Environ. Pollut.* **2018**, *241*, 775–786. [CrossRef]
12. Mądziel, M. Vehicle Emission Models and Traffic Simulators: A Review. *Energies* **2023**, *16*, 3941. [CrossRef]
13. Ma, X.; Lei, W.; Andréasson, I.; Chen, H. An Evaluation of Microscopic Emission Models for Traffic Pollution Simulation Using On-board Measurement. *Environ. Model. Assess.* **2012**, *17*, 375–387. [CrossRef]
14. U.S. Environmental Protection Agency. *User's Guide to MOBILE6.0: Mobile Source Emission Factor Model*; U.S. Environmental Protection Agency: Washington, DC, USA, 2002.
15. U.S. Environmental Protection Agency. *Overview of EPA's MOtor Vehicle Emission Simulator (MOVES3)*; U.S. Environmental Protection Agency: Washington, DC, USA, 2021.
16. Ntziachristos, L. *COPERT III Computer Programme to Calculate Emissions from Road Transport: Methodology and Emission Factors (Version 2.1)*; European Environment Agency: Copenhagen, Denmark, 2000.
17. André, M.; Keller, M.; Sjödin, Å.; Gadrat, M.; Mc Crae, I. The Artemis European tools for estimating the pollutant emissions from road transport and their application in Sweden and France. In Proceedings of the 17th International Conference Transport and Air Pollution, Graz, Austria, 16–17 June 2008.
18. Scora, G.; Barth, M. *Comprehensive Modal Emissions Model (Cmem), Version 3.01*; User Guide; Centre for Environmental Research and Technology, University of California: Riverside, CA, USA, 2006; Volume 1070, p. 1580.
19. Rakha, H.; Ahn, K.; Trani, A. Development of VT-Micro model for estimating hot stabilized light duty vehicle and truck emissions. *Transp. Res. Part D Trans. Environ.* **2004**, *9*, 49–74. [CrossRef]

20. Cappiello, A.; Chabini, I.; Nam, E.K.; Lue, A.; Abou Zeid, M. A statistical model of vehicle emissions and fuel consumption. In Proceedings of the IEEE 5th International Conference on Intelligent Transportation Systems, Singapore, 3–6 September 2002; pp. 801–809. [CrossRef]
21. Qi, Y.G.; Teng, H.H.; Yu, L. Microscale emission models incorporating acceleration and deceleration. *J. Transp. Eng.* **2004**, *130*, 348–359. [CrossRef]
22. Johnson, J.B. An Introduction to Atmospheric Pollutant Dispersion Modelling. *Environ. Sci. Proc.* **2022**, *19*, 18. [CrossRef]
23. Vardoulakis, S.; Fisher, B.E.A.; Pericleous, K.; Gonzalez-Flesca, N. Modelling air quality in street canyons: A review. *Atmos. Environ.* **2003**, *37*, 155–182. [CrossRef]
24. Benson, P.E. A review of the development and application of the CALINE3 and 4 models. *Atmos. Environ. Part B Urban Atmos.* **1992**, *26*, 379–390. [CrossRef]
25. Snyder, M.G.; Venkatram, A.; Heist, D.K.; Perry, S.G.; Petersen, W.B.; Isakov, V. RLINE: A line source dispersion model for near-surface releases. *Atmos. Environ.* **2013**, *77*, 748–756. [CrossRef]
26. Berkowicz, R.; Hertel, O.; Larsen, S.E.; Soerensen, N.N.; Nielsen, M. *Modelling Traffic Pollution in Streets*; Technical Report; National Environmental Research Institute: Copenhagen, Denmark, 1997.
27. Carruthers, D.J.; Holroyd, R.J.; Hunt, J.C.R.; Weng, W.S.; Robins, A.G.; Apsley, D.D.; Thompson, D.J.; Smith, F.B. UK-ADMS: A new approach to modelling dispersion in the earth's atmospheric boundary layer. *J. Wind Eng. Ind. Aerodyn.* **1994**, *52*, 139–153. [CrossRef]
28. Diegmann, V. *handbuch_immisluft_5_2.pdf*; IVU Umwelt GmbH: Breisgau, Germany, 2011.
29. Tominaga, Y.; Stathopoulos, T. Ten questions concerning modeling of near-field pollutant dispersion in the built environment. *Build. Environ.* **2016**, *105*, 390–402. [CrossRef]
30. Khan, B.; Banzhaf, S.; Chan, E.C.; Forkel, R.; Kanani-Sühring, F.; Ketelsen, K.; Kurppa, M.; Maronga, B.; Mauder, M.; Raasch, S.; et al. Development of an atmospheric chemistry model coupled to the PALM model system 6.0: Implementation and first applications. *Geosci. Model Dev.* **2021**, *14*, 1171–1193. [CrossRef]
31. Wendt, J. *Computational Fluid Dynamics: An Introduction*; Springer Science & Business Media: Berlin/Heidelberg, Germany, 2008.
32. Liang, M.; Chao, Y.; Tu, Y.; Xu, T. Vehicle Pollutant Dispersion in the Urban Atmospheric Environment: A Review of Mechanism, Modeling, and Application. *Atmosphere* **2023**, *14*, 279. [CrossRef]
33. Blocken, B. LES over RANS in building simulation for outdoor and indoor applications: A foregone conclusion? *Build. Simul.* **2018**, *11*, 821–870. [CrossRef]
34. Batterman, S.; Ganguly, R.; Harbin, P. High resolution spatial and temporal mapping of traffic-related air pollutants. *Int. J. Environ. Res. Public Health* **2015**, *12*, 3646–3666. [CrossRef] [PubMed]
35. Ioannidis, G.; Li, C.; Tremper, P.; Riedel, T.; Ntziachristos, L. Application of CFD Modelling for Pollutant Dispersion at an Urban Traffic Hotspot. *Atmosphere* **2024**, *15*, 113. [CrossRef]
36. Grumert, E.; Ma, X.; Tapani, A. Analysis of a cooperative variable speed limit system using microscopic traffic simulation. *Transp. Res. Part C Emerg. Technol.* **2015**, *52*, 173–186. [CrossRef]
37. Sanchez, B.; Santiago, J.L.; Martilli, A.; Martin, F.; Borge, R.; Quaassdorff, C.; de la Paz, D. Modelling NOX concentrations through CFD-RANS in an urban hot-spot using high resolution traffic emissions and meteorology from a mesoscale model. *Atmos. Environ.* **2017**, *163*, 155–165. [CrossRef]
38. San José, R.; Pérez, J.L.; Gonzalez-Barras, R.M. Assessment of mesoscale and microscale simulations of a NO_2 episode supported by traffic modelling at microscopic level. *Sci. Total Environ.* **2021**, *752*, 141992. [CrossRef]
39. Horni, A.; Nagel, K.; Axhausen, K.W. *The Multi-Agent Transport Simulation Matsim*; Ubiquity Press: London, UK, 2016. [CrossRef]
40. Maronga, B.; Banzhaf, S.; Burmeister, C.; Esch, T.; Forkel, R.; Fröhlich, D.; Fuka, V.; Gehrke, K.F.; Geletič, J.; Giersch, S.; et al. Overview of the PALM model system 6.0. *Geosci. Model Dev.* **2020**, *13*, 1335–1372. [CrossRef]
41. UC2. BMBF-Fördermaßnahme Stadtklima im Wandel. 2023. Available online: http://uc2-program.org/ (accessed on 9 January 2023).
42. Hülsmann, F.; Gerike, R.; Kickhöfer, B.; Nagel, K.; Luz, R. *Towards a Multi-Agent Based Modeling Approach for Air Pollutants in Urban Regions Entwicklung Eines Ansatzes zur Multi-Agentenbasierten Modellierung von Luftschadstoffemissionen in Urbanen Regionen*; Bundesanstalt für Straßenwesen: Bergisch Gladbach, Germany; FGSV Verlag GmbH: Cologne, Germany, 2011; pp. 144–166.
43. Kickhöfer, B.; Hülsmann, F.; Gerike, R.; Nagel, K. Rising car user costs: Comparing aggregated and geo-spatial impacts on travel demand and air pollutant emissions. In *Smart Transport Networks*; Edward Elgar Publishing: Cheltenham, UK, 2013; pp. 180–207. [CrossRef]
44. Notter, B.; Keller, M.; Althaus, H.J.; Cox, B.; Knörr, W.; Heidt, C.; Biemann, K.; Räder, D.; Jamet, M. *Handbuch Emissionsfaktoren des Strassenverkehrs*; Technical Report 4.1; INFRAS: Bern, Switzerland, 2019.
45. Agarwal, A. *Mitigating Negative Transport Externalities in Industrialized and Industrializing Countries*; Technische Universitaet Berlin: Berlin, Germany, 2017. [CrossRef]
46. Maronga, B.; Gross, G.; Raasch, S.; Banzhaf, S.; Forkel, R.; Heldens, W.; Kanani-Sühring, F.; Matzarakis, A.; Mauder, M.; Pavlik, D.; et al. Development of a new urban climate model based on the model PALM – Project overview, planned work, and first achievements. *Meteorol. Z.* **2019**, *28*, 105–119. [CrossRef]
47. Bresenham, J.E. Algorithm for computer control of a digital plotter. *IBM Syst. J.* **1965**, *4*, 25–30. [CrossRef]

48. Ziemke, D.; Kaddoura, I.; Nagel, K. The MATSim Open Berlin Scenario: A multimodal agent-based transport simulation scenario based on synthetic demand modeling and open data. *Procedia Comput. Sci.* **2019**, *151*, 870–877. [CrossRef]
49. Leich, G.; Nagel, K.; Rehmann, J.; Tilmann, S.; Martins-Turner, K.; Ziemke, D.; Castro, H.; Maciejewski, M.; Zilske, M.; Rakow, C.; et al. Matsim-Scenarios/Matsim-Berlin: Mosaik-2-01. 2023. Available online: https://doi.org/10.5281/zenodo.8319022 (accessed on 5 September 2023). [CrossRef]
50. Khan, B. Input Data for Performing Chemistry Coupled PALM Model System 6.0 Simulations with Different Chemical Mechanisms. 2020. Available online: https://publikationen.bibliothek.kit.edu/1000159940 (accessed on 20 September 2024). [CrossRef]
51. Senatsverwaltung für Mobilität, Verkehr, Klimaschutz und Umwelt. Berliner Luftgütemessnetz. Available online: https://luftdaten.berlin.de/station/overview/active (accessed on 2 January 2024).
52. Schümann, L.; Grunow, K.; Kaupp, H.; Clemen, S.; Kerschbaumer, A.; Rauterberg-Wulff, A. *Luftgütemessdaten Jahresbericht 2021*; Technical Report; Senatsverwaltung für Umwelt, Mobilität, Verbraucher- und Klimaschutz: Berlin, Germany, 2021.
53. DWD-Deutscher Wetter Dienst. Climate Data Center. Available online: https://cdc.dwd.de/portal/202209231028/mapview (accessed on 2 January 2024).
54. Alvarez Lopez, P.; Behrisch, M.; Bieker-Walz, L.; Erdmann, J.; Flötteröd, Y.P.; Hilbrich, R.; Lücken, L.; Rummel, J.; Wagner, P.; Wießner, E. Microscopic Traffic Simulation using SUMO. In Proceedings of the 2019 IEEE Intelligent Transportation Systems Conference (ITSC), Maui, HI, USA, 4–7 November 2018; IEEE: Piscataway, NJ, USA, 2018; pp. 2575–2582. [CrossRef]
55. EMEP/EEA. *Air Pollutant Emission Inventory Guidebook 2016: Technical Guidance to Prepare National Emission Inventories*; European Environment Agency: Copenhagen, Denmark, 2016.
56. José, R.S.; Pérez, J.L.; Morant, J.L.; González, R.M. CFD and Mesoscale Air Quality Modelling Integration: Web Application for Las Palmas (Canary Islands, Spain). In *Proceedings of the Air Pollution Modeling and Its Application XIX*; Springer: Dordrecht, The Netherlands, 2008; pp. 37–45. [CrossRef]
57. Smit, R.; Smokers, R.; Rabé, E. A new modelling approach for road traffic emissions: VERSIT+. *Transp. Res. Part D Trans. Environ.* **2007**, *12*, 414–422. [CrossRef]
58. Samad, A.; Caballero Arciénega, N.A.; Alabdallah, T.; Vogt, U. Application of the Urban Climate Model PALM-4U to Investigate the Effects of the Diesel Traffic Ban on Air Quality in Stuttgart. *Atmosphere* **2024**, *15*, 111. [CrossRef]
59. Chew, L.W.; Glicksman, L.R.; Norford, L.K. Buoyant flows in street canyons: Comparison of RANS and LES at reduced and full scales. *Build. Environ.* **2018**, *146*, 77–87. [CrossRef]
60. Zheng, X.; Yang, J. CFD simulations of wind flow and pollutant dispersion in a street canyon with traffic flow: Comparison between RANS and LES. *Sustain. Cities Soc.* **2021**, *75*, 103307. [CrossRef]
61. Laudan, J. MATSim Traffic Emission Module for PALM. 2023. Available online: https://zenodo.org/records/8319088 (accessed on 20 September 2024). [CrossRef]
62. Laudan, J. Mosaik-2 Simulation Experiment. 2023. Available online: https://depositonce.tu-berlin.de/items/bd40f70b-d194-49a2-a70c-8ec6db364c24 (accessed on 20 September 2024). [CrossRef]